

## Synoptic Circulation and Summertime Ground-Level Ozone Concentrations at Vancouver, British Columbia

IAN G. MCKENDRY

*Atmospheric Science Programme, Department of Geography, University of British Columbia, Vancouver, British Columbia, Canada*

(Manuscript received 10 June 1993, in final form 21 September 1993)

### ABSTRACT

The Kirchhofer synoptic classification procedure is applied to both mean sea level and 500-hPa NMC gridded pressure fields for the vicinity of southwestern British Columbia. Exceedances of the Canadian 1-h Ambient O<sub>3</sub> Air Quality Objective of 82 ppb at Port Moody, Vancouver, are associated with the coincidence of a low-level thermal trough and an upper-level ridge of high pressure. Analysis of synoptic sequences also reveals the importance of persistence in the development of elevated O<sub>3</sub> concentrations. The application of synoptic climatology to ground-level O<sub>3</sub> in Vancouver highlights the need for consideration of more than one atmospheric level in map-typing schemes. An extension of the basic Kirchhofer approach to permit multilevel computer-assisted map typing is advocated.

### 1. Introduction

Surface ozone (O<sub>3</sub>) is a secondary photochemical pollutant produced in the atmosphere by complex reactions between hydrocarbons and NO<sub>x</sub> emitted from a variety of natural and anthropogenic sources (notably motor vehicles). Day-to-day variations in O<sub>3</sub> may be attributed to variations in the rate, type, and sources of pollutant emissions as well as to the state of the atmosphere (Oke 1987). In particular, O<sub>3</sub> formation is affected not only by the mix of precursor species, but also by solar (UV) radiation, air temperature, wind, atmospheric stability, and inversion height (Comrie and Yarnal 1992).

In midlatitude regions, the meteorological variables that influence air quality are strongly modulated by the synoptic-scale circulation as manifested by the passage of fronts, cyclonic systems, and anticyclones. This has prompted the application of synoptic climatology to the investigation of day-to-day variations in air quality. Development of a synoptic climatology is generally defined as a two-stage process involving determination of a relatively small set of atmospheric circulation types (often on the basis of synoptic-scale weather maps), and secondly, the assessment of weather elements (or environmental variables) in relation to these classes (Barry and Perry 1973). Implicit in this procedure is the assumption that particular modes of atmospheric circulation produce distinctive environmental conditions at particular localities.

Three main approaches have been used to classify synoptic circulation types. The traditional subjective approach is labor intensive and involves the assignment of weather maps to predetermined classes on the basis of recognition of particular patterns (e.g., Comrie and Yarnal 1992). Multistage classification establishes weather types on the basis of a fixed order of procedures including principal components analysis (PCA), multiple regression analysis, and correlation analysis (e.g., Kalkstein and Corrigan 1986). Finally, computer-assisted weather typing by pattern correlation involves the application of simple linear regression correlation (the Lund method) or sum of squares (the Kirchhofer method) to gridded fields of pressure or geopotential height (e.g., Yarnal 1984b, 1985; Yarnal and White 1987; Yarnal et al. 1988).

El-Kadi and Smithson (1992), in a comparative review of synoptic typing procedures, recommend the Kirchhofer classification scheme as having important advantages to not only the subjective and PCA approaches, but also the Lund correlation method. Advantages include ease of application, the high proportion of days classified, and the reduced likelihood of intraclass variability. The latter arise from the consideration of not only overall map similarity but also the similarity of individual rows and columns of the set of grid points making up the map. Consequently, similarity in all areas of the grid is maintained.

To date, studies of the connections between surface O<sub>3</sub> and synoptic circulation have almost exclusively examined surface pressure patterns (e.g., Vukovich and Fishman 1986; Chung 1977), and the few studies that have adopted a synoptic climatological approach have utilized subjective surface pressure map-typing pro-

---

*Corresponding author address:* Dr. Ian G. McKendry, Department of Geography, University of British Columbia, #217-1984 West Mall, Vancouver, B.C., Canada V6T 1W5.

cedures (Comrie 1992; Comrie and Yarnal 1992; Heidorn and Yap 1986). In addition, these studies have focused almost exclusively on northeastern North America, where  $O_3$  episodes tend to be regional in scope and are generally associated with the western side of a slowly migrating high pressure system (Comrie and Yarnal 1992). In this regime, subjective map-typing procedures of mean sea level (MSL) pressure fields have exhibited satisfactory explanatory power.

By emphasizing surface pressure fields, the fundamentally three-dimensional nature of atmospheric processes is ignored in most studies. Clearly, the coupling of surface and upper-level flows has important air quality implications. For example, two days that may be represented by the same synoptic circulation type may be associated with quite different upper-level flow patterns. Consequently, these days may have quite different cloud patterns, wind and thermal regimes, and mixed-layer depths, all factors that may strongly influence ventilation and hence pollutant concentrations in the boundary layer. In typing procedures that utilize "clustering" of meteorological variables to produce circulation types, variables that reflect upper-level wind speeds and direction are easily incorporated (Ladd and Driscoll 1980). Subjective map-typing procedures may also take account of the coincidence of upper-level and surface circulation features in particular types (Ladd and Driscoll 1980; Heidorn 1989). However, the advent of computer-assisted map-typing procedures, as recommended by El-Kadi and Smithson (1992), has not yet produced a methodology that develops map-based circulation types reflecting flow patterns at more than one atmospheric level.

In this context, the present study has two principal goals:

- 1) To describe the relationship between synoptic-scale circulation and  $O_3$  concentrations in the Lower Fraser Valley (LFV) of southwestern British Columbia.

- 2) To demonstrate, using the example of the LFV, the importance of consideration of the three-dimensional structure of the atmosphere when applying computer-assisted map-typing schemes.

In so doing, the methodology described extends the innovative work of Yarnal (1984a,b) and Comrie (1992) and may promote improved explanation of the relationship between air quality and meteorological controls elsewhere. The study also documents a novel set of synoptic-mesoscale interactions responsible for elevated  $O_3$  concentrations.

## 2. Methods and data

### a. Synoptic climatology in the Pacific Northwest

Several precedents exist for application of the synoptic climatological approach in the Pacific Northwest. Maunder (1968), in a subjective synoptic climatology

of surface weather maps covering the Pacific Northwest and adjacent areas of the North Pacific for 1964 and 1965, identified seven patterns associated with surface high pressure systems (54% of days) and nine patterns associated with low pressure systems (38%). The remainder comprised a miscellaneous category. Of significance in this study was the importance of both the Alaskan low and the North Pacific high pressure systems and the seasonal variation in their influence.

Suckling and Hay (1978) also applied a synoptic classification approach in British Columbia with the objective of defining solar radiation regimes. Using the Lund correlation typing technique, they classified 1000-hPa height maps (113-point grid—average grid spacing 381 km) for the period 1963–72 into 28 principal types. With this approach 24% of days were unclassified. For the same 2-yr period used by Maunder (1968), Suckling and Hay (1978) classified 48% and 28% of days as being associated with anticyclonic and cyclonic conditions, respectively. The discrepancy between the two approaches was attributed to the coarse resolution of the gridded data used by Suckling and Hay (1978), which prohibited the identification of small cyclonic features in the vicinity of Vancouver Island.

More recently, Yarnal (1984a,b) utilized the Kirchhofer procedure to investigate the influence of synoptic variability in the National Meteorological Center (NMC) gridded 500-hPa height fields over the British Columbia region on glacial mass balances. In applying the Kirchhofer technique, Yarnal (1984b, 1985) also investigated the effects of map scale and interannual variability on the classification procedure. This important appraisal of sources of subjectivity in the Kirchhofer technique has been continued in the context of the midwestern United States (Yarnal and White 1987; Yarnal et al. 1988). In an analysis of 500-hPa patterns over the Pacific Northwest, Yarnal (1984b) identified 18 synoptic types, which accounted for 93.7% of the days.

### b. The classification procedure

In the present study, the Kirchhofer technique is applied to the Pacific Northwest region for daily MSL pressure and 500-hPa height fields for the period January 1978 to September 1992 (August 1992 for MSL). This period corresponds to the available  $O_3$  monitoring record for Vancouver. For the purposes of the general synoptic climatology, daily maps extending back to 1946 were also typed. The maps were derived from the NMC 1977-point octagonal grid of the Northern Hemisphere. Daily 1200 UTC synoptic MSL and 500-hPa weather maps for the Pacific Northwest were created by synthesizing a 36-point ( $6 \times 6$ ) latitude-longitude grid with mean grid spacing of approximately 350 km. The resulting grid (Fig. 1, inset), extending from  $42.5^\circ$  to  $55^\circ$ N and  $115^\circ$  to  $140^\circ$ W, was chosen to best represent synoptic patterns to the west and south

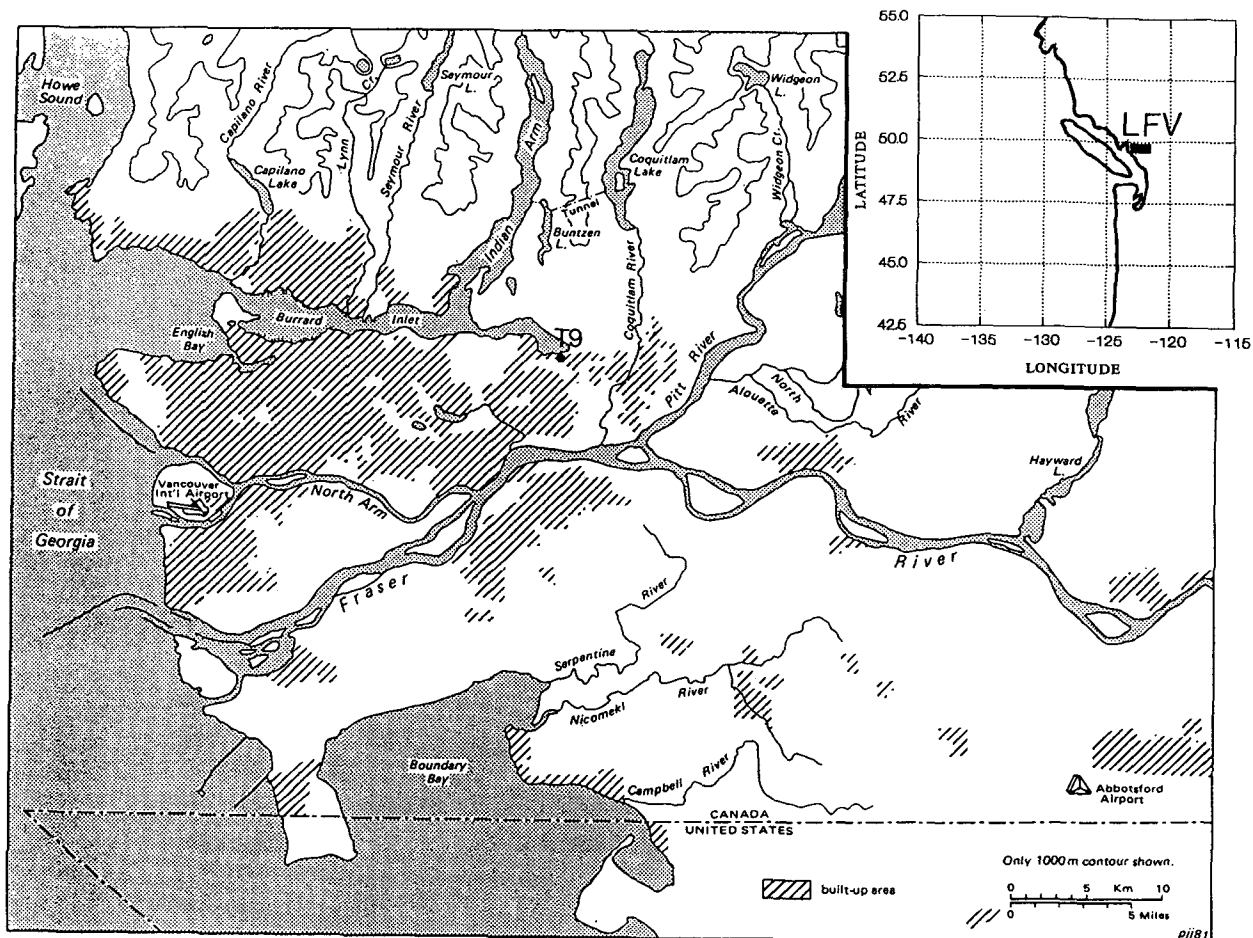


FIG. 1. Location of the Port Moody (T9) monitoring station within the Lower Fraser Valley (LFV). The 6 × 6 grid used in the synoptic typing procedure for the Pacific Northwest is inset. The LFV is highlighted to the east of Vancouver Island.

of the LFV (thereby capturing the northward extension of the surface thermal trough and subtropical high, and the eastward progression of upper-level ridges).

The Kirchhofer correlation-based (sum of squares) procedure was applied to the 500-hPa and MSL gridded fields in order to produce two separate classifications. In this procedure, each grid is first normalized in order to remove the effects of the seasonal cycle:

$$Z_i = \frac{x_i - \bar{x}}{s}, \tag{1}$$

where  $Z_i$  is the normalized value of grid point  $i$ ,  $\bar{x}$  the mean of the  $N$ -point grid, and  $s$  the standard deviation of the grid.

Due to computer storage limitations, a 5-yr sample (all days from 1984 through 1988) was then used to develop the synoptic classification and the key days required to classify both the MSL and 500-hPa datasets.

Each normalized grid in the sample was then compared to all other grids by the sum of squares equation:

$$S = \sum_{i=1}^N (Z_{ai} - Z_{bi})^2, \tag{2}$$

where  $S$  is the Kirchhofer score,  $Z_{ai}$  the normalized grid value of point  $i$  on day  $a$ ,  $Z_{bi}$  the normalized grid value of point  $i$  on day  $b$ , and  $N$  the number of data points. Days  $a$  and  $b$  represent any pair of maps for which the Kirchhofer score  $S$  is being calculated.

Subscore values for each row and column of the 6 × 6 matrices are also calculated using Eq. (2) in order to ensure pattern similarities in all areas of the grid.

Upper-level grids (500 hPa) are considered to be similar if  $S < 18$  (i.e.,  $0.5N$ ) and row and column scores  $S_R$  and  $S_C$  were less than  $1.0N_R$  and  $1.0N_C$ , where  $N_R$  and  $N_C$  equal the number of rows and columns in the grid, respectively (Yarnal 1985). MSL grids, with their greater spatial variability in fields, were considered similar if  $S < 1.0N$  (i.e., 36) and  $S_R$  and  $S_C$  were less than  $1.8N_R$  and  $1.8N_C$  (Yarnal 1985). This combi-

nation of thresholds gives approximately the same number of classes and percentages of days classified for 500-hPa and MSL pressure fields.

Within the 5-yr sample, the day that has the most  $S$  values associated with it (i.e., days meeting the threshold criteria) is designated key day 1. This key day is then removed from the analysis as are all grids associated with that key day and all days associated with those days. The analysis is then repeated with the reduced dataset to find key day 2, and so on, until all days are classified into  $m$  groups of 5 days or more. The remainder are deemed "unclassified."

Once the key days are established, Eq. (2) is then used to compare each of the key days with all grids (1946–92). Each day is then assigned to the class associated with the key day for which it produces the lowest  $S$  value.

### c. Ozone data

Southwestern British Columbia and western Washington State together from a complex coastal environment where local atmospheric circulations such as sea breezes and slope winds interact with synoptic-scale features (Mass 1982; Steyn and McKendry 1988). Within this climatic regime, summertime ground-level  $O_3$  concentrations often exceed the Canadian Ambient Air Quality Objective of 82 ppb (hourly) thereby creating a potential risk to human health and vegetation (notably crops). Previous studies in southwestern British Columbia (CSC 1985; Steyn et al. 1990; Taylor 1991, 1992) suggest that high  $O_3$  concentrations tend to be local in scope and associated with the coincidence of an upper-level ridge of high pressure (500 hPa) and a surface-based thermal trough that extends northward along the Pacific coast from the southwestern United States (Taylor 1991). This combination of lower- and midtropospheric flow patterns typically produces clear skies, warm air, and reduced mixing depths due to subsidence.

In order to investigate the relationship between synoptic circulation and tropospheric  $O_3$  in the LFV, data were utilized from a single station, located in Rocky Point Park (T9) alongside Burrard Inlet in the Port Moody Basin (Fig. 1). This station is designated as a National Air Pollution survey class I station and represents an area of particularly poor air quality in the LFV due to (a) its proximity to wood processing and coal-sulphur loading terminals, four petroleum refineries, and an intermittently used natural gas-fired power generator to the west, and (b) its position in an enclosed basin where dispersion is limited. The station is also considered to have the longest and most reliable record of stations in the LFV (Robeson and Steyn 1990). By choosing a station that has historically had a high frequency of exceedances (CSC 1985) of the 82-ppb Canadian Ambient Air Quality objective, the synoptic analysis is

intended to address the "worst case" scenario of poor air quality episodes in the LFV.

The time series of daily maximum  $O_3$  concentrations at Port Moody for the study period is shown in Fig. 2. Exceedances of the 82-ppb objective are strongly seasonal with virtually all occurrences occurring in the period May to September (inclusive). On average, the 82-ppb objective is exceeded on 8.7 days per year. There is considerable interannual variability in exceedances that may be attributed to synoptic meteorological variability, however. For example, the summer of 1988 produced unusually poor air quality both in the LFV and across North America, as a result of stagnating anticyclonic conditions induced by an amplified midcontinental ridge in the upper-level circulation (McKendry 1993). The high frequency of exceedances of the 82-ppb objective (some of very high magnitude) evident in the early portion of the time series (1978–81) is not so easily linked to meteorological conditions and may instead be associated with changing emission factors in the region.

## 3. Results

### a. Synoptic types

The classification procedure, as performed on the initial 1984–89 sample and then applied to the full 1946–92 dataset, produced 17 MSL and 18 500-hPa synoptic types accounting for 97.2% and 93.8% of total days, respectively. The remaining days were either missing or unclassified. The percentage frequencies associated with each class and the mean Kirchhofer scores (with standard deviations) are shown in Fig. 3. For both levels, mean Kirchhofer score  $S$  values are substantially below the threshold values (36 for MSL, 18 for 500 hPa). Together with relatively small standard deviations for the individual types, this suggests that the classification is relatively robust. The Kirchhofer scores are inversely proportional to frequency and indicate that there is more within-class variability in the less frequent pressure pattern types. Key day maps for the MSL and 500 hPa are shown in Figs. 4 and 5.

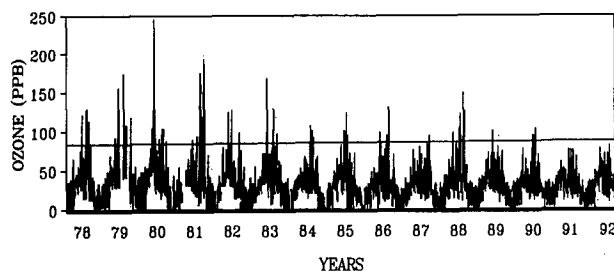


FIG. 2. Time series of daily 1-h maximum  $O_3$  concentrations at Port Moody.

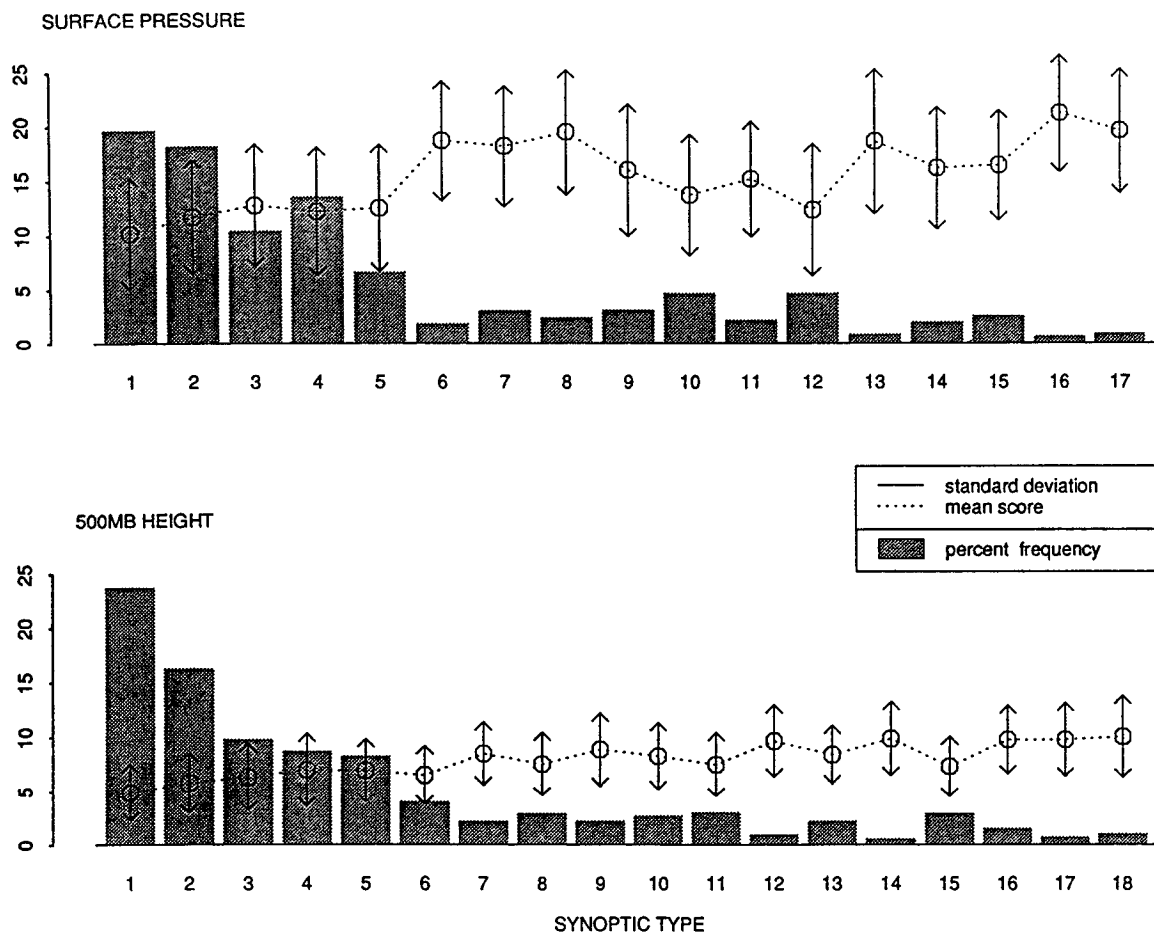


FIG. 3. Kirchofer scores with standard deviations and percentage frequencies for each synoptic type (MSL and 500 hPa) as classified for the 1946-92 period. The scale is common to all three variables plotted.

As an aid to explanation of links between synoptic conditions and ground-level  $O_3$  concentrations in the LFV, the large number of types identified may be subjectively grouped into a more manageable suite of types on the basis of broad commonalities. For the MSL classes, types are grouped according to the dominance of high and low pressure systems over the LFV (following Maunder 1968). For the purposes of the present study, a subgroup is also identified on the basis of the development of thermal trough that penetrates into the LFV from the south. The MSL groupings are

- thermal trough: types 5, 12, 13;  
 high dominant: types 1, 2, 3, 6, 7, 11, 15, 16, 17;  
 low dominant: types 4, 8, 9, 10, 14.

Similarly, the 500-hPa types may be grouped according to the presence and position of an upper-level ridge of high pressure, a feature considered to be of crucial importance to the development of  $O_3$  episodes (Taylor 1991; Steyn et al. 1990; CSC 1985). The 500-hPa groupings are

- ridge  $120^\circ$ - $130^\circ$ W: types 6, 8, 16;  
 ridge east of  $120^\circ$ W: types 1, 3, 10, 18;  
 ridge west of  $130^\circ$ W: types 2, 4, 7, 15;  
 no ridge: types 5, 9, 11, 12, 13, 14, 17.

These composite types are used below in the analysis of  $O_3$  concentrations.

#### b. Seasonal variations in synoptic circulation

In order to provide the necessary context for the ensuing discussion of summertime synoptic patterns and  $O_3$  concentrations, seasonal variations in the frequencies of the composite types described in the previous section are presented in Table 1. Seasons are defined in the meteorological sense with summer (June, July, August), autumn (September, October, November), winter (December, January, February), and spring (March, April, May).

Seasonal variability is evident in virtually all of the MSL types, especially those associated with the for-

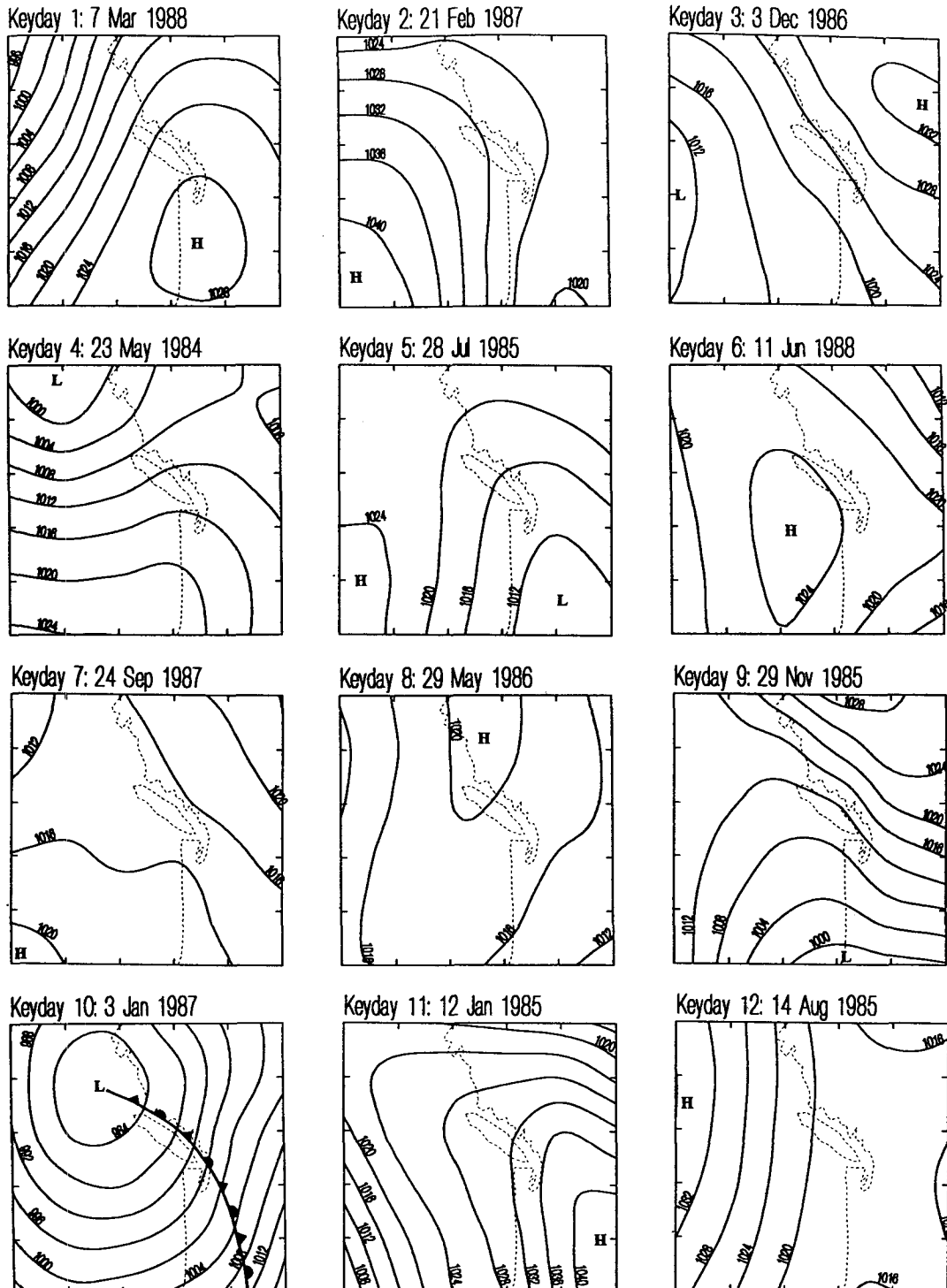


FIG. 4. Key days representing the 17 MSL synoptic types.

mation of a trough along the Pacific coast. The pronounced summer maximum in these types lends support to the view that such patterns are predominantly thermal in origin. Although the dominant high pressure

types in total do not display significant seasonal variability, there is a pronounced seasonal shift in the two most important types (1 and 2) with type 1 dominating in the cooler months and type 2 dominating in the

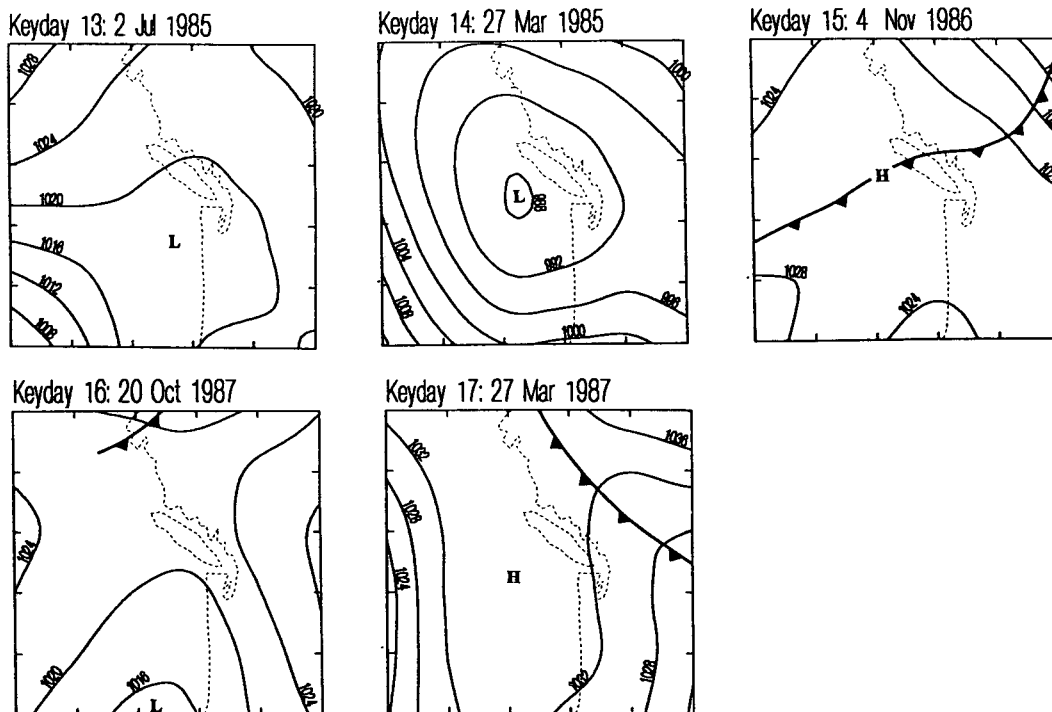


FIG. 4. (Continued)

summer. This reflects the seasonal shift in the strength and position of the north Pacific subtropical high. In the typical winter pattern (type 1), the subtropical high extends a ridge of high pressure along the west coast of the continent. The northward movement and strengthening of this feature in summer produces the typical summer pattern (type 2) in which high pressure pushes into British Columbia from the southwest. As expected, dominant low pressure types generally show a summer minimum (due to the dominating influence of the subtropical high) and a winter maximum. For the entire dataset, dominant low pressure types account for 26% of days. This compares favorably with values of 38% and 28% determined by Maunder (1968) and Suckling and Hay (1978), respectively (both studies were based on two years of data and different classification techniques).

At 500 hPa, marked seasonal variations are also apparent in the frequency of synoptic types. High pressure ridges developed between 120° and 130°W are most frequent in winter and least frequent in summer. Ridges positioned to the west or east show little seasonal variability while the nonridge patterns have a summer maximum with frequencies twice that of the winter. These patterns reflect seasonal variations in the character of upper-level long-wave patterns in the Northern Hemisphere. In winter, the midlatitude westerlies at 500 hPa are at a maximum (reflecting the strong thermal gradient between the poles and equator) and the mean flow pattern is strongly asymmetric with deep

troughs over eastern North America (and on average a ridge over the Rockies) and Asia. In summer, with a weaker temperature gradient between the poles and equator the hemispheric pattern is more symmetric (zonal) and the predominant midlatitude westerlies weaker. Over the west coast of North America, this weakened zonal flow results in a higher frequency of troughs aligned along the coast in summer (Barry and Perry 1973). In the present analysis, this pattern is apparent in the high summer frequencies of 500-hPa types 5 and 9, both of which show a trough of low pressure at 500 hPa aligned along the British Columbia coast.

Having provided the synoptic context, the remaining discussion will focus on the relationship between daily maximum O<sub>3</sub> concentrations (hourly) at Port Moody and synoptic types for the monitoring period 1978–92 and for the months May to September (inclusive).

### c. Synoptic-scale circulation and O<sub>3</sub> concentrations

Mean maximum daily O<sub>3</sub> concentrations (with standard deviations) for each synoptic type are shown in Figs. 6a,b. For MSL synoptic types, below-average concentrations are strongly associated with the dominant low pressure types (10, 4, and 14) in which a center of low pressure is located close to, or to the northwest, of Vancouver Island. The two other dominant low pressure types (8 and 9) are associated with above-average O<sub>3</sub> concentrations. In both these situa-

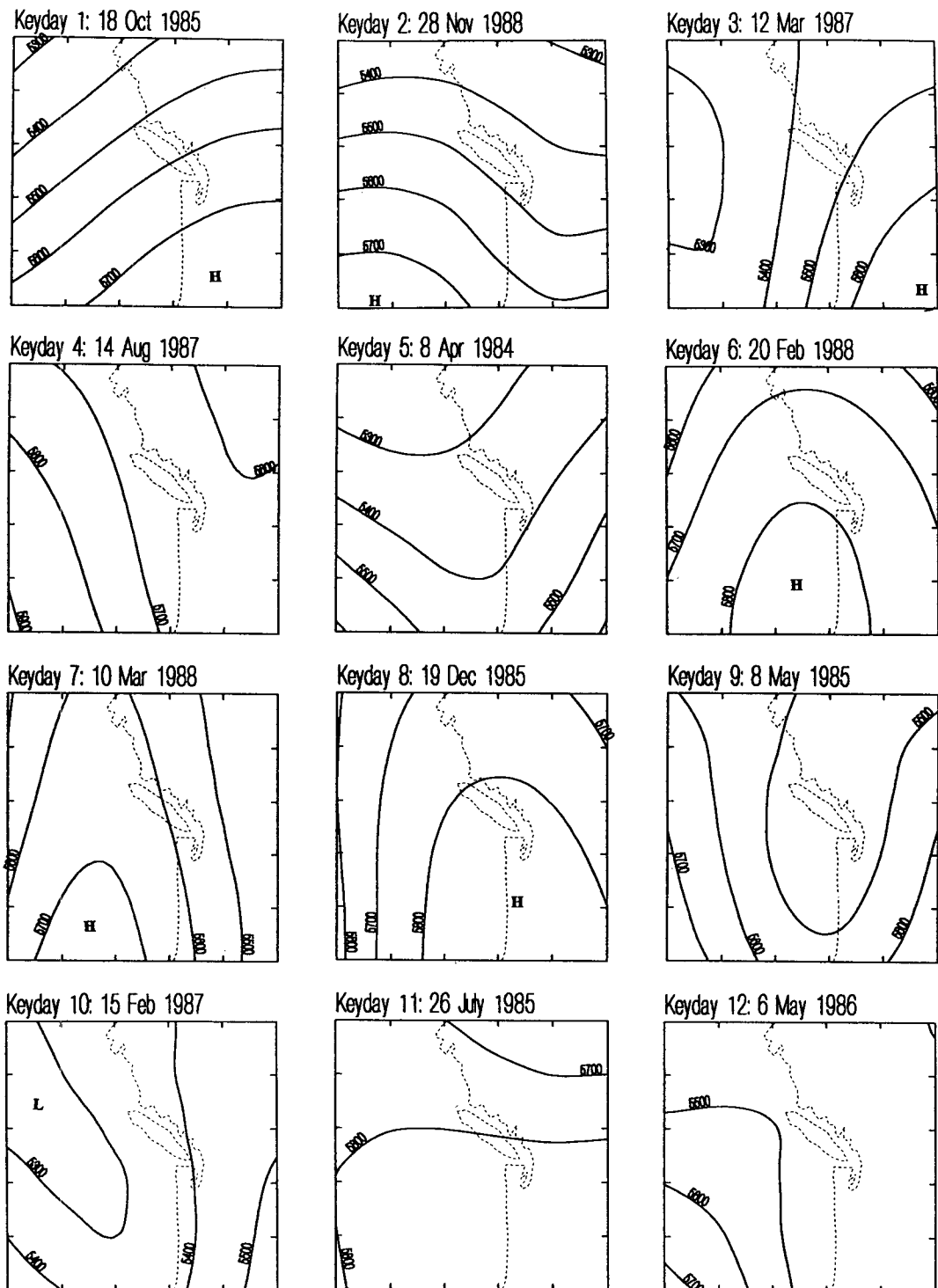


FIG. 5. Key days representing the 18 500-hPa synoptic types.

tions, the dominant low pressure center (and associated fronts) is located at some distance from the LFV (to the northeast or south) and hence the synoptic state is relatively undisturbed. Above-average maximum daily

$O_3$  concentrations are associated with dominating high pressure and in particular with the presence of a thermal trough along the coast (5, 12, and 13). Type 13, a relatively infrequent type (23 days in total 1978–92),



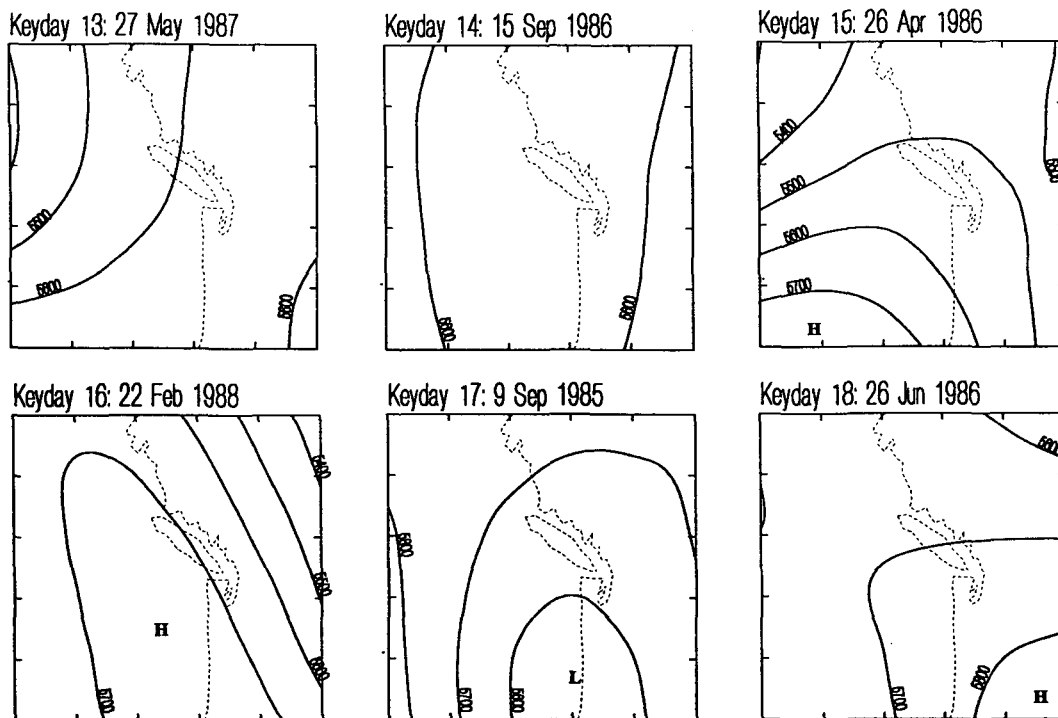


FIG. 5. (Continued)

has the highest mean O<sub>3</sub> concentrations of all classes. This type is characterized by a very slack pressure gradient over southern British Columbia and a weak thermal trough along the coast.

At 500 hPa (Fig. 6b), the location and presence of an upper-level ridge appears to be an important factor contributing to above-average daily maximum O<sub>3</sub> concentrations. Highest mean concentrations are all associated with an upper-level ridge aligned along the Pacific Northwest coast between 120° and 130°W (types 16, 6, and 8). With the ridge located to the west of 130°W (15, 2, and 4), upper-level flow tends to be

northwesterly in direction and mean O<sub>3</sub> concentrations are generally below average. Higher concentrations occur when the ridge is located east of 120°W (especially types 1 and 3). In this situation, upper-level southwesterly flow is responsible for the advection of warm air into the region. When there is no ridge present, O<sub>3</sub> concentrations are generally below average. Exceptions are types 11 and 13. In both cases, the upper-level gradients are very weak as a result of a split in the upper-level flow.

Hitherto, MSL and 500-hPa patterns have been considered separately. A simple cross tabulation of the frequencies of MSL and 500-hPa types reveals that MSL types are associated with a wide range of 500-hPa types and vice versa. Furthermore, when mean O<sub>3</sub> concentrations and weather conditions are calculated for each combination of MSL and 500-hPa types, it is apparent that for any particular upper-level type, O<sub>3</sub> concentrations and mean weather conditions may vary considerably depending on the surface flow pattern. Highest mean O<sub>3</sub> concentrations tend to be associated with a relatively small number of specific MSL–500-hPa combinations. For example, in Fig. 7, mean O<sub>3</sub> concentrations and weather conditions are presented for the 11 MSL types that occur in combination with 500-hPa type 3, an upper-level ridge located to the east of the LFV. Mean concentrations greater than 60 ppb are most frequently associated with this upper-level flow pattern and occur particularly in combination with

TABLE 1. Percentage frequencies of MSL and 500-hPa composite types by season (1946–92). Columns sum to 100% for each map level.

	Spring	Summer	Autumn	Winter
<b>MSL type</b>				
Trough	11.8	20.7	9.8	6.1
Dominant high	57.8	57.8	59.7	62.3
Dominant low	27.2	18.2	27.9	29.1
Unclassified	3.1	3.2	2.5	2.5
<b>500-hPa type</b>				
Ridge 120°–130°W	7.7	5.4	9.1	11.7
Ridge east of 120°W	35.8	37.2	38.5	33.4
Ridge west of 130°W	28.7	25.6	32.7	33.4
No ridge	19.7	24.4	15.4	12.3
Unclassified	8.0	7.4	4.3	4.9

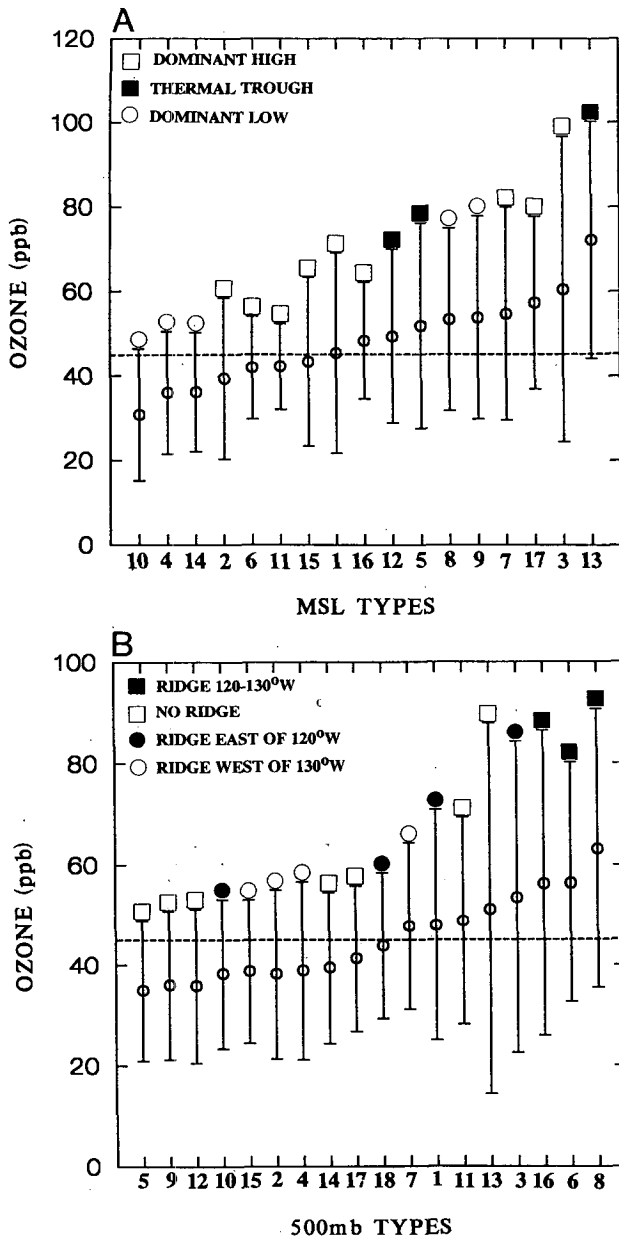


FIG. 6. Mean (with standard deviation bars) daily maximum ozone concentrations at Port Moody 1978-92 (May-September) by (a) MSL and (b) 500-hPa synoptic types.

an MSL trough along the coast (MSL types 5, 7, 9, and 13). The mean concentration of 82 ppb associated with the combination of type 3 at 500 hPa and type 13 at MSL is the highest for the entire cross tabulation of MSL and 500-hPa types.

A salient feature of the combinations having high mean O<sub>3</sub> concentrations is a tendency for high maximum daytime temperatures, low precipitation, and westerly winds at Vancouver International Airport (e.g., type 13 in Fig. 7). Such conditions are typically

linked to the development of the summer sea breeze in the LFV (Steyn and Faulkner 1986). In contrast, lowest O<sub>3</sub> concentrations are associated with cyclonic conditions (e.g., MSL types 10 and 14) in which maximum temperatures are lower, and cloud cover, precipitation, and wind speeds greater.

*d. Synoptic sequences and O<sub>3</sub> concentrations*

The sequencing method of Comrie (1992) permits investigation of the extent to which elevated O<sub>3</sub> concentrations in the LFV may be attributed to the evolution of synoptic patterns over time scales of 2-3 days. Underpinning this approach is the notion that both the trajectory and speed of systems across the region will influence the extent to which O<sub>3</sub> concentrations may "build up" under conditions of reduced ventilation. In this approach, each day is ascribed a three-number code representing the synoptic types for 2, 1, and 0 days before the day in question. For example, "2, 4, 5" represents a 3-day sequence with the end day (day 0) being synoptic type 5 and having a particular maximum daily O<sub>3</sub> concentration that contributed to the average O<sub>3</sub> concentration for this particular sequence. Consequently, the number of 3-day sequences is equal to the number of days in the dataset. For all sequences identified, mean daily O<sub>3</sub> concentrations on day 0 were determined.

In summary, the patterns in synoptic sequences reflect the tendency established in Fig. 6a for highest O<sub>3</sub> concentrations to be associated with dominant high pressure and the presence of a thermal trough. Con-

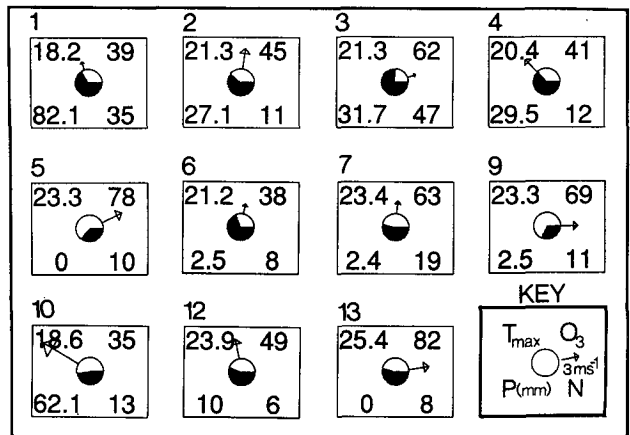


FIG. 7. Mean weather conditions at Vancouver International Airport and mean daily maximum ozone concentrations at Port Moody for MSL types associated with 500-hPa type 3 (May-September 1978-92). Clockwise from the top-right quadrant are mean daily maximum O<sub>3</sub> concentration, the mean daily maximum temperature, the daily precipitation (mm), and the number of days contributing to the averages. The unshaded portion of the center circle represents the percentage of daylight hours during which there was bright sunshine. The wind vector emanating from the center circle depicts the mean wind vector at 1500 LST at Vancouver International Airport.

versely, lowest concentrations are associated with MSL sequences ending in days characterized by dominant low pressure. In addition, the analysis highlights the extent to which persistence is an important factor in producing high daily maximum concentrations. For example, MSL sequences 12, 12, 5 and 5, 5, 5 represent persistent thermal troughs along the Pacific coast and are associated with mean O<sub>3</sub> concentrations of the order of 60 ppb. However, the more frequent pattern (2, 2, 5), representing a developing thermal trough, only has average daily maximum concentrations (~44 ppb). Similarly, the sequences ending in synoptic type 13 produce highest concentrations (89 ppb) when the type has persisted for more than 1 day. In a separate 500-hPa analysis, highest concentrations are also associated with a sequence characterized by persistence of a particular weather type; a 500-hPa ridge of high pressure between 120° and 130°W. Sequences ending in a ridge of high pressure to the west or no ridge at all produce a cluster of O<sub>3</sub> concentrations below the overall mean value.

*e. Composite sequences producing elevated O<sub>3</sub> concentrations*

In order to generalize the results of the sequencing analysis to days on which the 82-ppb standard was exceeded at Port Moody, composite MSL and 500-hPa map sequences for 2, 1, and 0 days before the day of exceedance were produced for each of the MSL types associated with O<sub>3</sub> exceedances. These 12 sequences were then subjectively grouped into two main types (56 and 52 cases, respectively) and a single subtype (7 cases) on the basis of obvious similarities in the fields (both MSL and 500 hPa) and the dynamic evolution of the sequences. Three new composite map sequences were then compiled (Figs. 8a–c). By comparing each of the contributing maps to the composite, using the basic Kirchhofer procedure described in section 2b, a measure of the “significance” of the composite maps can be determined. Table 2 shows mean Kirchhofer scores  $S$  and standard deviations of  $S$  ( $\sigma_s$ ), and the percentage of days satisfying the Kirchhofer threshold for the suite of days contributing to each composite map. Low mean Kirchhofer scores and low standard deviations suggest strong similarity between maps contributing to the composite. Mean values greater than the threshold  $S$  values (18 for 500 hPa, 36 for MSL) suggest variability between maps that is greater than that between maps within the original synoptic types discussed in section 3a and summarized in Fig. 3. It is worth noting that of the 115 exceedances contributing to the composite maps, 59% were not preceded by exceedances on the prior 2 days, while 27% and 14% also had exceedances 1 and 2 days prior to the exceedance, respectively. Although there is some overlap inherent in the compositing procedure (i.e., the composite map 1 day prior to the “day of exceedance” also includes

TABLE 2. Kirchhofer statistics for composite maps (Pct represents proportions of days contributing to maps that meet Kirchhofer thresholds,  $S$  the Kirchhofer score, and  $N$  the number of maps contributing to the composite).

Type and day	MSL				500 hPa				
	$N$	$S$	$\sigma_s$	Pct	$N$	$S$	$\sigma_s$	Pct	
A	-2	56	20.1	20.9	75	53	19.6	13.3	45
	-1	56	19.8	20.5	77	51	21.2	13.1	33
	0	56	13.2	8.7	91	50	18.5	15.2	50
B	-2	52	31.0	19.3	46	48	13.4	11.4	69
	-1	52	28.9	19.3	54	52	12.9	12.5	71
	0	52	22.0	14.7	69	52	9.9	12.3	77
C	-2	7	35.4	26.6	43	7	17.7	8.7	43
	-1	7	20.5	25.4	86	7	12.7	9.0	57
	0	7	22.0	14.7	100	7	10.5	11.8	71

some exceedances of the 82-ppb threshold), the results are unlikely to be significantly biased, given the low proportion of multiday episodes and the persistent nature of the patterns.

The type A pattern (Fig. 8a) representing 47% of exceedances during the 1978–92 period, is characterized by a slowly evolving synoptic pattern in which an MSL thermal trough builds along the coast of the Pacific Northwest in the presence of a ridge of high pressure extending from the subtropical anticyclone. This pattern is virtually identical to that identified by Taylor (1991). At 500 hPa, the pattern involves the eastward migration of the upper-level ridge to a position directly over the coast. Taylor (1991) suggests that this development is responsible for the advection of warm subtropical air northward, and hence, the northward extension of the MSL thermal trough. MSL Kirchhofer scores for each of the days contributing to this sequence are well below the threshold value (36) with 91% of days contributing to composite map “day 0” satisfying the threshold. As might be expected, days contributing to the sequence 2 days prior to the exceedance tend to exhibit more variability. At 500 hPa, the type appears to be less coherent with mean  $S$  scores slightly above the threshold value and only a maximum of 50% of contributing maps satisfying the criterion. This suggests that the crucial element contributing to an O<sub>3</sub> exceedance in type A is the slowly evolving surface pressure pattern in association with an upper-level ridge that may show some variability in terms of position and strength. Certainly, in the 1–5 September 1988 episode of elevated O<sub>3</sub> concentrations described in Steyn et al. (1990), the MSL sequence was virtually identical to the type A MSL sequence shown here. However, at 500 hPa the ridge that developed shifted further to the east and was stronger than that shown in the composite.

Station circles depicting the mean weather conditions at Vancouver International Airport and the mean daily maximum O<sub>3</sub> concentrations at Port Moody are

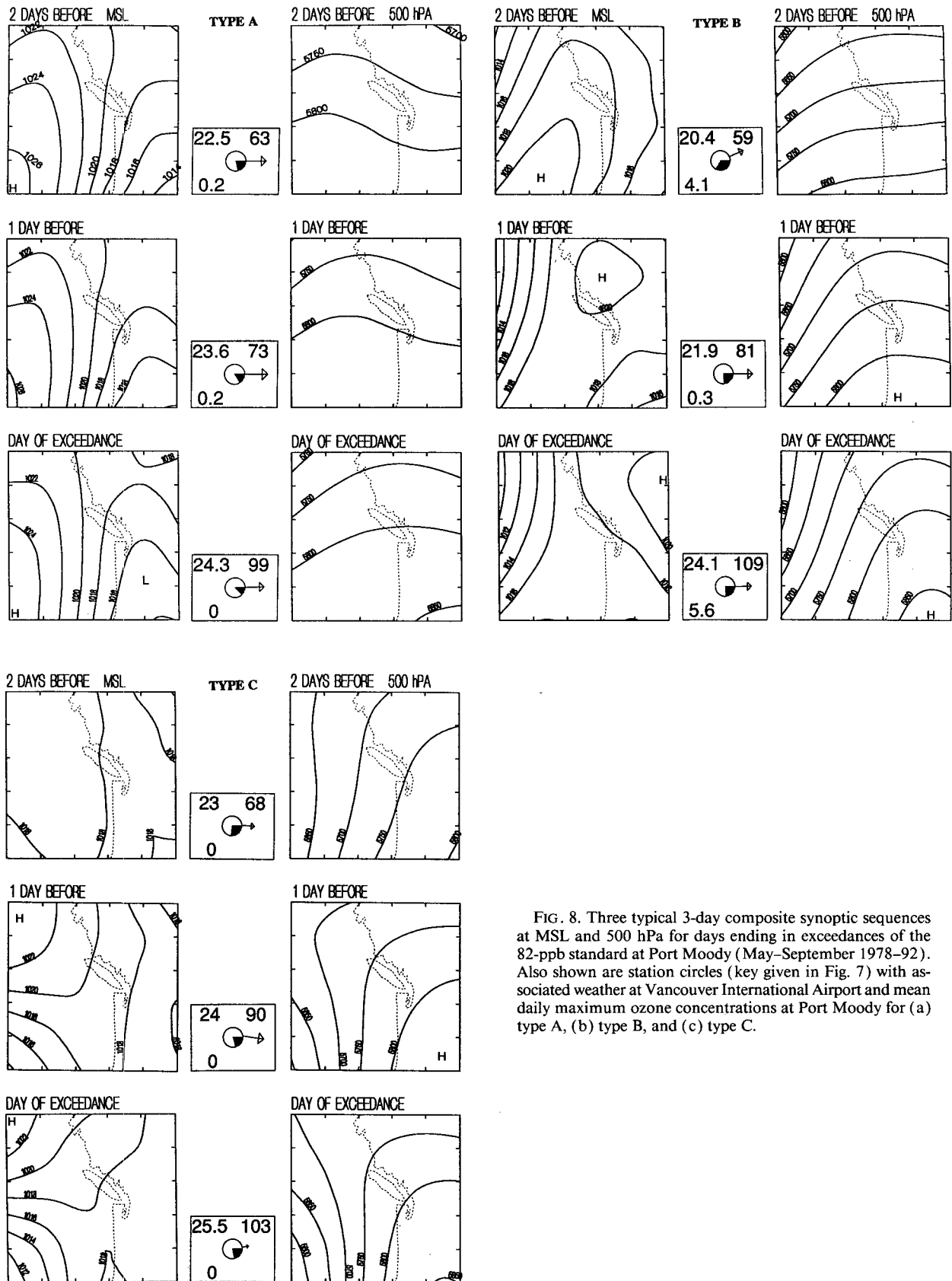


FIG. 8. Three typical 3-day composite synoptic sequences at MSL and 500 hPa for days ending in exceedances of the 82-ppb standard at Port Moody (May–September 1978–92). Also shown are station circles (key given in Fig. 7) with associated weather at Vancouver International Airport and mean daily maximum ozone concentrations at Port Moody for (a) type A, (b) type B, and (c) type C.

also shown on the composite maps. For the type A sequence, mean daily maximum O<sub>3</sub> concentrations increase steadily throughout the sequence (99 ppb on the day of exceedance) under relatively clear skies and increasing daily maximum temperatures. By the final day of the sequence, mean maximum daily temperatures at Vancouver International Airport are close to the 25°C threshold for O<sub>3</sub> exceedances identified by CSC (1985). Midafternoon wind directions at Vancouver International Airport are consistently westerly throughout the sequence and show a tendency for winds to be lightest on the last day of the sequence. This pattern is consistent with Taylor's (1991) suggestion that the development of a thermal trough along the coast of the LFV inhibits the mesoscale sea breeze that typically develops on sunny warm days and is responsible for the predominance of summertime westerly winds at Vancouver International Airport (Steyn and Faulkner 1986; Steyn and McKendry 1988).

The second pattern identified (type B) represents 44% of the exceedances in the region and is characterized by a more dynamic pattern than that shown for type A. The MSL sequence shows a weak pressure gradient over the region and in contrast to the previous type, a major low pressure center to the west of Vancouver Island. The development of the latter feature appears to "squeeze" out the ridge of high pressure over southwestern BC that is well developed 2 days before the exceedance. A weak trough of low pressure is evident along the Washington coast by day "0." Examination of the maps contributing to this composite suggest a strong tendency for the gradient MSL flow over the LFV to veer from the northwest to the southeast during the sequence. This contrasts with the previous type where the gradient MSL flow remains northeasterly throughout the sequence. At 500 hPa, a strong upper-level ridge builds to a position to the east of the LFV. In this pattern, the Kirchhofer statistics suggest that the 500-hPa sequence represents a good statistical "fit" with all *S* scores well below the threshold (18) and more than 70% of days meeting the threshold value. Although the MSL patterns meet the threshold requirements, fewer days qualify and Kirchhofer statistics are higher than for type A. This may be attributed to the larger number of day "0" types contributing to this composite sequence (6) than for type A (3). The statistics also suggest that the dominant element in type B exceedances is the evolution of the upper-level pattern, which advects warm subtropical air into the region.

Local climatic conditions associated with the type B pattern exhibit many similarities to those discussed above in relation to the type A sequence. Mean daily maximum temperatures increase throughout the sequence and bright sunshine is recorded at Vancouver International Airport for approximately 75% of possible hours. Furthermore, midafternoon winds appear to decrease on the day of the exceedance. Mean O<sub>3</sub> con-

centrations at Port Moody rise more rapidly than in the type A type reaching an average of 109 ppb on the final day of the sequence.

The final pattern identified (type C) is represented by only seven cases (6% of exceedances) and therefore it is not statistically significant. The type shows persistent southerly gradient flow at 500 hPa associated with a ridge of high pressure over eastern British Columbia. At MSL, the pressure gradients are extremely weak and the sequence relatively static. Maximum daily temperatures throughout the sequence are consistently high, once again under predominantly clear skies with no precipitation.

The three major patterns presented show many similarities in terms of the local weather associated with sequences and the broad synoptic-scale features. Common to each is the development of a coastal thermal trough of low pressure in conjunction with a ridge of high pressure at 500 hPa. The development of the trough appears to be inextricably linked to warm air advection associated with southwesterly flow on the upstream side of the ridge. In each type, the development of the trough appears to inhibit the strength of the local sea breeze, thereby reducing ventilation and presumably allowing concentrations to increase over the western portion of the LFV. Further research is required to investigate the links between the sea breeze and this low-level thermal trough. In summary, the three sequences identified seem to represent subtypes of a basic pattern characterized by slack MSL pressure gradients and the simultaneous development of a ridge aloft and a surface thermal trough. The individual types vary on the basis of the position and strength of the ridge aloft, the dominance of the subtropical high, and the evolution of the patterns over the 3-day period.

#### 4. Discussion and conclusions

Summertime daily maximum O<sub>3</sub> concentrations in Vancouver appear to be strongly modulated by the synoptic-scale atmospheric circulation. This is not surprising. As studies elsewhere have shown, synoptic conditions that produce clear skies, warm air, light winds, and reduced mixing depths promote reduced air quality. What is significant in the Pacific Northwest is that such conditions are associated not with a stagnating surface anticyclone (as in eastern North America), but with the development of a low-level thermal trough in combination with an upper-level ridge. By adopting a synoptic climatological approach, the present analysis provides confirmation and further explanation of the patterns previously identified in case studies as being deleterious to air quality in southwestern British Columbia (Steyn et al 1990; Taylor 1991).

The critical importance of coupling between the surface and upper-level flow patterns to O<sub>3</sub> concentrations in the LFV suggests that traditional synoptic cli-

matological approaches that emphasize classification of a single atmospheric level (usually the surface) within a static framework have limited air quality applications. The present analysis highlights the extent to which particular surface circulation types may be associated with a wide range of 500-hPa types. Consequently, only by explicit consideration of the three-dimensional structure of the atmosphere can the meteorological controls on O<sub>3</sub> concentrations be satisfactorily explained. Furthermore, the LFV example confirms that meteorological controls on air quality can only be examined within a dynamic framework. Elevated O<sub>3</sub> concentrations appear to be strongly controlled by antecedent synoptic conditions and the degree of persistence in the evolving synoptic state. Within this context, the sequencing and compositing techniques developed by Comrie (1992) are particularly useful. Scope exists for further refinement of the synoptic climatological approaches to air quality analysis described here, however. In the present study, a qualitative approach was used to identify three subclasses of the basic pattern that results in elevated O<sub>3</sub> concentrations. This source or subjectivity in the analysis could perhaps be removed by adoption of a more sophisticated statistical approach.

Furthermore, in view of the added explanation provided by consideration of both surface and 500-hPa fields, it is proposed that the Kirchhofer classification procedure be extended to explicitly incorporate more than one atmospheric level. A particular circulation type would then represent a single configuration of upper and lower flow patterns. Assuming availability of sufficient computational resources, this could be achieved by minor modification of the method outlined in section 2b to allow simultaneous comparison of both surface and 500-hPa fields for a particular day with all other days. In addition, days allocated to particular types must meet the threshold requirements for surface and 500-hPa fields, respectively. Maintenance of a manageable number of types would be a major challenge in such an approach and may require judicious relaxation of the thresholds for Kirchhofer scores. Although considerable refinement of the basic methodology may be required to produce a classification that successfully incorporates more than one atmospheric level, it is likely that such a typing procedure would not only prove fruitful in air quality applications, but also provide added explanation in other applications of synoptic climatology.

Despite the relatively successful application of the Kirchhofer procedure in the Vancouver context, it is imperative to recognize that applications of synoptic climatology to air quality will always be constrained by meteorological subtleties that cannot be resolved by consideration of synoptic fields alone. In the LFV, the position, movement, and strength of the thermal trough, the strength and inland penetration of the sea breeze, as well as a host of precursor emission factors,

contribute to significant variations in air quality within particular synoptic types. From a forecasting perspective, this suggests that while recognition of synoptic patterns and sequences conducive to elevated concentrations will be useful, predictions must also be based on accurate photochemical models as well as detailed mesoscale meteorological analysis and emissions information.

*Acknowledgments.* This research was completed as part of a British Columbia Ministry of Environment contract. I am grateful to Drs. Dan Moore, Tim Oke, and Douw Steyn for useful comments on the manuscript. Special thanks also go to Many Li-Ting-Wai for the computational work.

#### REFERENCES

- Barry, R. G., and A. H. Perry, 1973: *Synoptic Classification, Methods and Applications*. Methuen, 555 pp.
- Chung, Y. S., 1977: Ground-level ozone and regional transport of air pollutants. *J. Appl. Meteor.*, **16**, 1127-1136.
- Comrie, A. C., 1992: An enhanced synoptic climatology of ozone using a sequencing technique. *Phys. Geog.*, **13**, 53-65.
- , and B. Yarnal, 1992: Relationships between synoptic-scale atmospheric circulation and ozone concentrations in metropolitan Pittsburgh, Pennsylvania. *Atmos. Environ.*, **26B**, 301-312.
- Concord Scientific Corporation, 1985: Vancouver Oxidants Study Air Quality Analysis Update 1982-84, Prepared for Environment Canada, Environmental Protection Service, 86 pp. [Available from CSC, 2 Tippett Rd., Toronto, Ontario, Canada M3H 2V2.]
- El-Kadi, A. K. A., and P. A. Smithson, 1992: Atmospheric circulations and synoptic climatology. *Prog. Phys. Geogr.*, **16**, 432-455.
- Heidorn, K. C., 1989: A synoptic climatology of southwestern Ontario with applications to surface ozone concentrations. Ph.D. thesis, Columbia Pacific University. [Available from University Microfilms, Inc., Ann Arbor, Michigan.]
- , and D. Yap, 1986: A synoptic climatology for surface ozone concentrations in southern Ontario, 1976-1981. *Atmos. Environ.*, **20**, 695-703.
- Kalkstein, L. S., and P. Corrigan, 1986: A synoptic climatology approach for geographical analysis: Assessment of sulphur dioxide concentrations. *Ann. Assoc. Am. Geogr.*, **76**, 381-395.
- Ladd, J. W., and D. M. Driscoll, 1980: A comparison of objective and subjective means of weather typing: An example from West Texas. *J. Appl. Meteor.*, **19**, 691-704.
- Mass, C., 1982: The topographically forced diurnal circulations of western Washington State and their influence on precipitation. *Mon. Wea. Rev.*, **110**, 170-183.
- Maunder, W. J., 1968: Synoptic weather patterns in the Pacific Northwest. *Northwest Sci.*, **42**, 80-88.
- McKendry, I. G., 1993: Ground-level ozone in Montreal, Canada. *Atmos. Environ.*, **27B**, 93-103.
- Oke, T. R., 1987: *Boundary Layer Climates*. 2d ed. Methuen, 435 pp.
- Robeson, S. M., and D. G. Steyn, 1990: Evaluation and comparison of statistical forecast models for daily maximum ozone concentrations. *Atmos. Environ.*, **24B**, 303-312.
- Steyn, D. G., and D. A. Faulkner, 1986: The climatology of sea-breezes in the Lower Fraser Valley. *B. C. Clim. Bull.*, **20**(3), 21-39.
- , and I. G. McKendry, 1988: Quantitative and qualitative evaluation of a three-dimensional mesoscale numerical model simulation of a sea breeze in complex terrain. *Mon. Wea. Rev.*, **116**, 1914-1926.
- , A. C. Roberge, and C. Jackson, 1990: The anatomy of an extended air pollution episode in British Columbia's Lower Fraser Valley. Report prepared for Waste Management Branch,

- BCME, 55 pp. [Available from British Columbia Ministry of Environment, 777 Broughton St., Victoria, British Columbia, Canada V8V 1X5.]
- Suckling, P. W., and J. E. Hay, 1978: On the use of synoptic weather map typing to define solar radiation regimes. *Mon. Wea. Rev.*, **106**, 1521-1531.
- Taylor, E., 1991: Forecasting ground-level ozone in Vancouver and the Lower Fraser Valley of British Columbia, Report PAES-91-3, Scientific Services Division, AES, Pacific Region, EC, 8 pp. [Available from Atmospheric Environment Service, Pacific Region, Environment Canada, 1200 West 73rd Ave., Vancouver, British Columbia, Canada.]
- , 1992: The relationship between ground-level ozone concentrations, surface pressure gradients and 850 mb temperatures in the Lower Fraser Valley of British Columbia. Atmospheric Issues and Services Branch, Atmospheric Environment Service, Pacific Region, Environment Canada, 7 pp. [Available from Atmospheric Environment Service, Pacific Region, Environment Canada, 1200 West 73rd Ave., Vancouver, British Columbia, Canada.]
- , 1984a: A procedure for the classification of synoptic weather maps from gridded atmospheric pressure surface data. *Comput. Geosci.*, **10**, 397-410.
- , 1984b: The effect of weather map scale on the results of a synoptic climatology. *J. Climatol.*, **4**, 481-493.
- , 1985: A 500 mb synoptic climatology of Pacific Northwest coast winters in relation to climatic variability, 1948-49 to 1977-1978. *J. Climatol.*, **5**, 237-252.
- , and D. A. White, 1987: Subjectivity in a computer-assisted synoptic climatology. I: Classification results. *J. Climatol.*, **7**, 119-128.
- , —, and D. J. Leathers, 1988: Subjectivity in a computer-assisted synoptic climatology. II: Relationships to surface climate. *J. Climatol.*, **7**, 227-239.